Environmental Science Nano

ROYAL SOCIETY OF CHEMISTRY

PAPER

View Article Online
View Journal | View Issue

Cite this: *Environ. Sci.: Nano*, 2025, **12**, 4966

Soil-based zeolite and metal oxide nanomaterial application alters reactive nitrogen losses and lettuce (*Lactuca sativa* L.) growth

Jessica J. Chadwick, *[a] Iuliia Mikulska,[b] Aleksandar Radu,[c] Swaroop Chakraborty,[a] Peng Zhang,[a] Sami Ullah[a] and Iseult Lynch *[a]

Received 3rd June 2025,
Accepted 24th September 2025

DOI: 10.1039/d5en00526d

rsc.li/es-nano

Excessive nitrogen fertiliser use has resulted in reactive nitrogen losses to the environment through gaseous N emissions, like N_2O, resulting in agriculture being a major anthropogenic source of N_2O gas emissions globally. Using engineered nanomaterials to deliver reactive nitrogen can aid in more efficient nutrient delivery to crops, maximising yield and crop quality, while minimising reactive losses to the environment. ZSM-5-15, a nano-zeolite, increased cumulative N_2O emissions by 134% when applied in combination with a 50% dose of conventional nitrogen fertiliser. This is theorised to be through ion exchange of ZSM-5-15's extra-framework NH_4^+ ion load being released, allowing nitrifying microbes to act on the newly released NH_4^+ and increase N_2O emissions. BEA-19, a similar zeolite to ZSM-5-15 but with a slightly altered Si : Al ratio, size and charge, causes no increase in N_2O emissions. While ZSM-5-15 increases reactive N emissions it also drives improved lettuce growth, with 13% more biomass accumulation compared to a half dose of conventional fertiliser. $Ce_{0.75}Zr_{0.25}O_2$, a nano-metal oxide, improves growth by 6% and maintains the nutritive quality of lettuce, with higher Zn, Cu, Mg, K, Fe and Mn contents, without increasing N_2O emissions. Nano-$Ce_{0.75}Zr_{0.25}O_2$ transforms in soil to form CeO_2 and $Ce_{0.9}Zr_{0.1}O_2$, leaching Zr^{4+} ions some of which form $ZrCl_4$. These compounds may then act on lettuce roots and soil microbes independently. These results indicate how nanomaterials may impact reactive nitrogen emissions through effects on soil microbial communities.

Environmental significance

With rising interest in the application of nanomaterials within agriculture, the broader effects of engineered nanomaterials on soils are increasingly of interest. Many nanomaterial studies are performed in pristine environments, however research on nanomaterial mobility and transformation in soil is essential for biologically relevant understanding. This research explores the effects of two soil applied nano-zeolites and a mixed metal oxide on soil N-cycling and lettuce growth as a holistic approach. Research on nanofertilisers often assesses soil functioning indicators like microbial diversity or activity, but lacks consideration of potential impacts on soil nutrient cycling. Here we show that highly differential effects can occur even between nanomaterials of similar compositions and characteristics, and that N-cycling measurements are critical in ensuring safe and sustainable nano-enabled agriculture.

1. Introduction

Since the discovery of the Haber–Bosch process in 1913 the total input of reactive nitrogen (Nr) into agricultural ecosystems has more than doubled due to excessive use of synthetic fertiliser.[1] Increased fertiliser use has supported global food security and human population growth, with over half of the world's current population reliant on nitrogen (N) fertiliser produced food.[2] Synthetic fertiliser has permitted an increase in crop productivity, low uptake efficiencies from soils (by crops) have enriched agricultural soils with Nr thus resulting in its loss to the environment through aqueous run-off and gaseous emissions. These losses include gaseous N compounds that contribute to climate change, primarily through the production of N_2O, which has a global warming potential (GWP) of ~300 as compared to carbon dioxide (CO_2) and whose atmospheric concentration has increased to 332 ppb in 2021, compared to pre-industrial levels of 275 ppb.[3] Other volatile N compounds include ammonia (NH_3) and nitrogen oxides (NO_x), that are formed through different stages of N transformations and contribute to climate change as well as impacting air quality. There are

[a] *School of Geography, Earth and Environmental Sciences, University of Birmingham, Edgbaston, Birmingham B15 2TT, UK.*
E-mail: jessicajchadwick@gmail.com, i.lynch@bham.ac.uk
[b] *Diamond Light Source Ltd, Harwell Science & Innovation Campus, Didcot, Oxfordshire OX11 0DE, UK*
[c] *School of Chemistry, University of Lincoln, Lincoln LN6 7TS, UK*

also Nr losses through run-off and groundwater leaching in the form of nitrate (NO_3^-) and ammonium (NH_4^+), contributing to eutrophication and reducing water quality. It is essential to reduce the impact of synthetic fertiliser on the environment without compromising crop productivity, the ability of global agriculture to support the population, and the livelihoods of farmers.

Nanomaterials (NM) have been posited as a solution for precision agriculture, aiding in efficient nutrient delivery and promoting crop growth and stress tolerance. NMs have at least one dimension between 1 and 100 nm, with a huge surface area to volume ratio permitting environment-dependent transformations (amongst other qualities). NM function is highly dependent on their characteristics, including size, shape, surface charge and chemistry, which in turn alter their reactivity, adsorption/binding kinetics and mobility.[4–6] The dynamic nature of NMs (as indicated by their propensity to transform) presents a challenge, as generalisations about the behaviour and impacts of different classes of NMs are difficult to make, with changes in shape, size and constituent element ratio altering their fate and effects significantly.[7] This is particularly true in biological systems. Soil is a highly heterogeneous environment, and NM interactions with minerals, organic matter and microorganisms can trigger ion dissociation and biotransformation of the NMs.[7,8] Similarly, plants with their varied solute concentrations and highly specialised internal environments, further alters NM transformations, resulting in highly specific interactions between NMs, soil types and plant species.[9,10] NM introduction to the soil environment causes changes to the physicochemical properties of NMs, altering NM behaviour, fate, and biological activity, with NMs impacted by soil pH, organic matter and water content.[11,12] These in turn can cause NM agglomeration, transformation, adsorption to the soil matrix or other compounds present and influence NM dissolution, having further impacts on NM behaviour as well as on nutrient supply, including N. Characterising NMs in soil and plants is a further challenge due to the difficulties in tracing the NMs through the whole agricultural system and the requirement that NMs are dispersed for most characterisation methods and in many cases separated from the complex environmental matrix.[13]

Previous research indicates that NM application is able to reduce the nitrogen, phosphorus and potassium (NPK) input needs of crop plants, with metallic NMs shown to impact the cycling of N, P and C.[14,15] Here, research is focussed on three metallic NMs, two nano-zeolites, BEA-19 and ZSM-5-15, and a mixed metal oxide, $Ce_{0.75}Zr_{0.25}O_2$. Zeolites are highly porous aluminosilicates; their porosity lends itself to specific ion exchange capabilities, making them useful catalysts. In particular, metal-exchanged ZSM-5 NMs have been used in nitrous oxide (N_2O) decomposition.[16] Previous research has shown that nanoceria (CeO_2) and nano-zirconium oxide (ZrO_2) both have antioxidative properties,[17] with significant research already exploring the application of CeO_2 NMs to different crops.[18–20] The mixed metal oxide utilised here is $Ce_{0.75}Zr_{0.25}O_2$, which follows the nanostructure $Ce_{1-x}Zr_xO_2$. Previous research has utilised $Ce_{0.75}Zr_{0.25}O_2$ NMs as catalysts due to their high dynamic oxygen exchange capacity.[21,22] This catalytic activity may enable them to function as nanozymes, directly mimicking the action of biological enzymes in the soil to minimise gaseous N emissions.[23]

The experiments presented herein aimed to investigate how soil-based NM application with reduced NPK fertiliser input affected crop growth and yield and soil N gaseous fluxes. The hypothesised mechanism is that binding of the NPK nutrients to the surface of the NMs results in a binding dynamic that allows slow nutrient release and, due to the NMs ability to cross biological barriers and be taken up into plants, would allow a more direct nutrient release, thereby minimising the potential for nutrient losses to the environment. Parameters studied include biomass as a measure of plant growth, antioxidative response to assess NM toxicity or stress initiation to aid in deciphering NM mechanism of action, and elemental analysis in order to determine how NM application altered macro- and micronutrient accumulation in lettuce tissue and if there was above-ground accumulation of the NMs based on analysis of their constituent elements. To understand the nutrient cycling that occurred, CO_2, N_2O and NH_3 gas fluxes were captured *via* gas sampling and analysis. Nitrate, phosphate and ammonium content of the soil and leachate were also analysed to determine how the nutrient supply was influenced by NMs and fertilization. X-ray absorption spectroscopy (XAS) was utilised to determine $Ce_{0.75}Zr_{0.25}O_2$ NM transformations in the soil environment over the timescales of the exposure and uptake by plants. Analysis of the NMs transformations was performed to better understand the mechanisms driving the NMs impacts in the environment and to determine in what form the NMs are when they interact with, or enter, plant tissues. We hypothesized that NM co-application with a reduced dose of fertiliser (half of the conventional dose) would be able to maintain lettuce yield with a reduction in N emissions from soil as a result.

2. Materials and methods

2.1. Materials

An aqueous dispersion of $Ce_{0.75}Zr_{0.25}O_2$, was obtained from Promethean Particles (UK) *via* the NanoSolveIT project. Powdered ZSM-5-15 (Si/Al = 15.0) and BEA-19 (Si/Al = 19.0) were obtained from Zeolyst (USA). Hydrodynamic diameter and zeta potential were determined using 500 mg L^{-1} NM dispersions in deionised water using a dynamic light scattering (DLS) instrument (Zetasizer, Malvern Instruments, UK). NPK treatment comprised of urea (Sigma-Aldrich) and potassium phosphate monobasic (Sigma-Aldrich). Primary particle size information on BEA-19 was sourced from Jendrlin *et al.*,[24] on ZSM-5 from Song *et al.*[25] and on $Ce_{0.75}Zr_{0.25}O_2$ from Dhage *et al.*[26]

2.2. Greenhouse study, sampling and analysis

The soil used in the study was collected from FarmED (coordinates 51.869981, −1.581136, **https://www.farm-ed.co.uk/**) where the loam soil had an oolitic limestone bedrock and a 30 year history of conventional wheat and barley planting. The soil was collected in September 2022 with previous cultivation including barley from March–August 2022. Soils were watered to 60% water holding capacity (WHC) with regular water additions of 100–300 mL per 1.5 kg of soil to maintain soil moisture throughout the experiment. Details of the water chemistry (chemical analysis) are listed in full in the Table S1.

Soils were sieved to 2 mm before 1.5 kg (dry weight) soil was brought back to 60% WHC and left to rest under greenhouse conditions (21 °C, 16:8 light/dark cycle) for one week. Soil pH and electrical conductivity (EC) was recorded before any treatments were applied and the soil was found to be pH 8.1 and 149 μS cm^{-1}. After the seven days the soils were treated with either NPK, a combination of half concentration of NPK and NM suspension, or water as a control. In the case of the NM treatments a 25 mg kg^{-1} NM suspension was added to 100 mL of deionised water along with an NPK treatment made from urea and potassium phosphate monobasic. The NM treatment concentration was determined through literature review to be a relatively low NM concentration, minimising the risk of negative ecological impacts, that was still present at sufficient levels to be detectable in the soil.[27] The full NPK treatment consisted of 180 kg hm^{-2} N, 200 kg hm^{-2} of P_2O_5 and K_2O based on the UK DEFRA RB209A fertiliser manual. The application rates used are recommended for a loamy soil with the previous growing season having been used for winter wheat with an average organic matter content of 3–4%.[28] The reduced fertilisation was half NPK treatment and consisted of 90 kg hm^{-2} N and 100 kg hm^{-2} of P_2O_5 and K_2O. *Lactuca sativa* L. seeds ("Tom Thumb" variety; Premier Seeds Direct Limited, UK) were sterilised using 1.5% NaClO solution for 10 minutes before rinsing with deionised water until odourless. Five seeds were sown directly in the treated or untreated soils and grown for eight weeks in a greenhouse at 21 °C with 16:8 hour light to dark day cycles. After the first week post-sowing, similarly sized seedlings were maintained (>2 cm tall) and the rest removed from each pot replicate, to leave one seedling per pot. Lettuce growth was monitored through height and width measurements and leaf counts over the course of the eight-week experiment. The lettuce's fresh biomass was weighed at the end of the eight-week growing period before being snap frozen using liquid nitrogen and stored at −80 °C for future analyses.

2.3. Soil characterisation and net nitrogen mineralisation

Soils were characterised before and after the 8 week experiment for gravimetric soil moisture, pH and EC. The soil samples were kept after the experiments and stored in a cold room at 4–7 °C. Gravimetric soil moisture was calculated using a 5 g soil subsample that was weighed before and after 24 h drying at 105 °C. Soil extraction for nitrate, ammonium and phosphate analysis was done using 2 M KCl with a 1 : 10 ratio between sieved soil and the KCl solution. The mixture was shaken for one hour at 200 rpm at room temperature before being centrifuged and the supernatant filtered using 0.45 μm syringe filters. The extractant was stored at −20 °C before use. Net nitrogen mineralisation was studied for each biological replicate at the end of the eight-week experiment by incubating 20 g of soil at room temperature in the dark for 28 days before extraction as detailed prior. The post incubation soil extractants were then compared to the end of growth period soil extractions to assess how much nitrogen was nitrified. Dried soil samples underwent elemental analysis and were digested for analysis by inductively coupled plasma optical emission spectroscopy (ICP-OES) as described below.

2.4. Greenhouse gas fluxes

Static chamber gas sampling with gas chromatography was performed to measure N_2O and CO_2 emissions. Static chambers had dimensions 15 × 20 × 20 cm and were sealed at the base with water to ensure they were airtight. 15 mL of gas samples were taken at 0 hours, 0.5 hours, 1 hour and 2 hours on a weekly basis and stored in 12 mL pre-evacuated exetainer vials (Labco Limited, UK). The gas samples were analysed using the Agilent 7890A Gas Chromatograph (GC) interfaced with a PAL3 autosampler (Agilent Technologies Ltd, USA) following the method used in Comer-Warner *et al.*[29] and using reference standards as described in Sgouridis and Ullah.[30] Every 20 samples a standard (N_2O = 0.2 ppm, CH_4 = 4 ppm, and CO_2 = 500 ppm) was used to prevent drift with minimum detectable concentration differences of 9 ppb N_2O, 72 ppb CH_4 and 31 ppm CO_2. GC analysis of N_2O used a micro electron capture detector (μECD), while a flame ionisation detector (FID) was used to analyse CH_4 and CO_2 methanised into CH_4.

A 1 M H_2SO_4 solution with 2% (w/v) glycerol was used as an acid trap for ammonia emissions from the soils. The acid trap was incubated inside the static chambers for two hours during the weekly gas sampling. The acid trap solution was then extracted with deionised water before NH_4^+ analysis *via* the ISO/DIS 15923-1 standard analysis method on an AQ400 Discrete Analyser (SEAL Analytical, WI, USA).

2.5. Soil and lettuce analyses

2.5.1 Soil nutrient analysis. Soils in the pots containing the growing lettuce plants were watered with 100–300 mL per pot to reach 60% WHC, and a funnel was used to capture the first 50 mL of resulting leachate on weeks 1, 2, 4 and 8. The funnel was washed with deionised water between replicates and treatments. This leachate was filtered using a 0.45 μm syringe filter and stored at −20 °C until preparation for analysis within a week of sampling date. Leachate and KCl extracted soil samples were analysed for nitrate, ammonium

and orthophosphate concentration using a Tecan Spark microplate reader (Tecan, UK). Ammonium analysis was performed in accordance with the Mulvaney[31] protocol. Samples and reagents for the ammonium assay were incubated at 40 °C for 15 minutes, returned to room temperature, and absorbance readings were taken at 650 nm. Nitrate concentrations were determined using a VCl_4 based method.[32] Microplates underwent a 6–12 hour incubation at 4 °C before an absorbance reading was taken at 540 nm. The phosphate assay was performed as described by Murphy and Riley.[33] The microplate was incubated for 10 minutes at room temperature before taking an absorbance reading at 880 nm. Each assay used their respective standard solutions which were made up in the same extractant background as the samples, KCl or tap water.

2.5.2 Macro- and micronutrients, NM constituent elements and plant stress marker analysis. Samples (lettuce and soil) were digested for inductively coupled plasma optical emission spectroscopy (ICP-OES) according to the protocols for spinach tissue and the US EPA 3052 protocol for soil/sediment as described in the MARS 6 Microwave Acid Digestion Method Note Compendium.[34] Digestion program details are displayed in full in Tables S2 and S3. Resulting digestate was diluted 50-fold before running samples on the Perkin Elmer optima 8000 ICP-OES for analysis (Agilent Technologies Ltd, USA). The elements studied were P, K, Zn, Ca, Mg, Fe and Mn, as well as the NM constituent elements Ce, Zr, Al and Si. Both dried soil samples and freeze-dried lettuce tissue samples underwent elemental analysis (EA) for C, N, and S. EA details are elaborated on in the SI. Frozen lettuce tissues were used for a malondialdehyde (MDA) assay which measures lipid membrane peroxidation as a marker for oxidative stress (Sigma-Aldrich, UK). The assay was performed according to the manufacturer's instructions.

2.6. X-ray absorption spectroscopy

Soil samples spiked with 3000 mg kg^{-1} $Ce_{0.75}Zr_{0.25}O_2$ NMs were used for X-ray absorption spectroscopy (XAS) analysis. Soils were treated with the NMs dispersion and mixed thoroughly, followed by 8 weeks of incubation at 21 °C. 200 mg soil samples were pelleted for analyses, with XAS spectra collected on beamline B18 (ref. 35 and 36) at the Diamond Light Source synchrotron radiation facility (Didcot, UK). Zr K-edge XAS spectra on soil samples were collected in fluorescence mode using a Canberra 36-pixel monolithic segmented hyper pure germanium detector (HPGe) with Xspress4 signal processing,[37] while Ce L_{III}-edge spectra were collected in fluorescence mode using Vortex-ME4 silicon drift detector partnered with the Xspress3 digital pulse processor. Details of XAS spectra collection for experimental samples, reference compounds and reference foils are in the SI. Demeter software package was used to perform the data analysis, including energy calibration, normalisation and linear combination fitting (LCF) analysis.[38]

2.7. Statistics

R Statistical Software was used for all analyses.[39] Data was initially assessed for normality using Shapiro–Wilk tests, *Q–Q* plots and homogeneity of variance testing. Where normality was breached, non-parametric statistical analyses were performed. Kruskal–Wallis tests, followed by Dunn's *post hoc* test for pairwise comparison were performed for the soil samples. Normally distributed data were analysed with one-way ANOVA, followed by *post hoc* Tukey HSD (honest significant difference) tests. GC calculated N_2O and CO_2 concentrations, and leachate nutrient concentrations, were assessed using linear mixed models to interrogate treatment and time effects on emissions. *Post hoc* comparisons of linear mixed model results were evaluated using Tukey tests. Lettuce biomass comparisons were performed using Bonferroni corrected two-sample *t*-tests comparing control lettuce with all other treatments. The threshold for statistical significance was set at $p = 0.05$.

3. Results

500 mg L^{-1} NMs dispersed in water showed both zeolites as negatively charged (Table 1) with BEA-19 having a more negative zeta potential than ZSM-5-15. The $Ce_{0.75}Zr_{0.25}O_2$, however, was positively charged. The three pristine NMs also had varying agglomerate sizes as determined *via* DLS, with BEA-19 agglomerates the largest and $Ce_{0.75}Zr_{0.25}O_2$ NMs the smallest.

BEA-19 primary particle size was found to be 0.05 μm, as measured by SEM or TEM.[24] According to Jendrlin *et al.*,[24] ZSM-5 particles were 0.2 μm. Another paper found Zeolyst sourced ZSM-5-15 particles to be 32 nm, with larger aggregates found between 700–1000 nm (25). $Ce_{0.75}Zr_{0.25}O_2$ primary particle size was found to be 5 nm using TEM.[26] The SEM and TEM derived particle sizes makes it clear that the NMs are agglomerated, and that the hydrodynamic size values are thus for the NM aggregates.

Soil moisture varied across treatments, with the control soil having greater moisture levels than BEA-19 ($p = 0.02$), $Ce_{0.75}Zr_{0.25}O_2$ ($p = 0.0041$), and ZSM-5-15 ($p = 0.00061$) treated soils. Additionally, soil moisture was significantly lower in ZSM-5-15-treated soils than that of NPK full ($p = 0.01$) (Table 2). Soil pH varied across treatments, with NPK full soil pH being significantly lower than in $Ce_{0.75}Zr_{0.25}O_2$ treated soil ($p = 0.0052$) or NPK half treated soil ($p = 0.01$). The positively charged $Ce_{0.75}Zr_{0.25}O_2$ NMs had a particularly alkalinizing effect on the soil, producing a significantly

Table 1 Nanomaterial characterisation using dynamic light scattering (DLS) before exposure to soil. Data are means ± standard deviation

Nanomaterial	Mean hydrodynamic size (nm) ($n = 3$)	Mean zeta potential (mV) ($n = 3$)
BEA-19	997.8 (± 196.8)	−39.5 (± 0.95)
ZSM-5-15	631.3 (± 12.7)	−28.0 (± 0.66)
$Ce_{0.75}Zr_{0.25}O_2$	104.5 (± 4.37)	+45.2 (± 0.75)

Table 2 Soil properties in the six different soil treatments after the eight-week growth period. Data are means ± standard error. Absent data is due to values being below the limit of detection of the specific method. NPK is the standard recipe of the synthetic fertilizer, nitrogen, phosphorus, potassium, and half NPK is half of the standard dosage

Soil properties	Control	NPK full	NPK half	BEA-19 + NPK half	$Ce_{0.75}Zr_{0.25}O_2$ + NPK half	ZSM-5-15 + NPK half
Gravimetric soil moisture (%) (n = 4)	73.9 (± 1.1)	69.9 (± 2.9)	66.3 (± 1.6)	63.1 (± 1.5)	60.9 (± 1.2)	58.2 (± 3.2)
pH (n = 4)	8.31 (± 0.06)	6.84 (± 0.18)	8.82 (± 0.05)	8.65 (± 0.07)	8.86 (± 0.04)	8.60 (± 0.09)
EC (μS cm^{-1}) (n = 4)	49.5 (± 3.3)	76.4 (± 8.5)	52.1 (± 2.6)	60.0 (± 10.5)	46.2 (± 4.9)	39.5 (± 2.0)
NO_3^- (mg kg^{-1} dry soil) (n = 4)	2.81 (± 0.43)	9.14 (± 2.59)	4.02 (± 1.15)	5.70 (± 2.73)	3.29 (± 1.09)	1.82 (± 0.39)
Post-incubation NO_3^- (mg kg^{-1} dry soil) (n = 4)	0.789 (± 0.33)	11.7 (± 1.85)	3.28 (± 1.54)	4.36 (± 2.06)	1.80 (± 0.68)	0.934 (± 0.056)
PO_4^{3-} (mg kg^{-1} dry soil) (n = 4)	—	0.01 (± 0.0041)	0.0017 (± 0.0007)	0.00081 (± 0.0002)	0.00065 (± 0.00024)	0.0012 (± 0.00026)
N (%) (n = 4)	0.26 (± 0.01)	0.28 (± 0.02)	0.28 (± 0.01)	0.28 (± 0.01)	0.27 (± 0.004)	0.28 (± 0.01)
C (%) (n = 4)	5.89 (± 0.34)	5.89 (± 0.41)	6.28 (± 0.02)	5.98 (± 0.13)	6.07 (± 0.02)	6.02 (± 0.21)
C : N (n = 4)	22.8 (± 0.3)	20.9 (± 0.7)	22.3 (± 1.0)	21.8 (± 0.7)	22.5 (± 0.6)	21.4 (± 0.8)
K (mg kg^{-1} dry soil) (n = 4)	8469 (± 311)	8396 (± 368)	7913 (± 257)	7838 (± 254)	9734 (± 1147)	8497 (± 268)
P (mg kg^{-1} dry soil) (n = 4)	1170 (± 85)	1270 (± 93)	1158 (± 39)	1105 (± 26)	1364 (± 93)	1095 (± 55)
Cu (mg kg^{-1} dry soil) (n = 4)	26.0 (± 6.7)	15.8 (± 1.9)	25.7 (± 6.7)	55.4 (± 3.7)	43.4 (± 1.5)	84.8 (± 7.3)
Al (mg kg^{-1} dry soil) (n = 4)	18 916 (± 416)	17 482 (± 339)	17 962 (± 613)	15 010 (± 585)	21 291 (± 4932)	16 687 (± 291)
Si (mg kg^{-1} dry soil) (n = 4)	170 418 (± 7860)	160 528 (± 13 517)	151 159 (± 8819)	146 620 (± 5459)	156 984 (± 7853)	173 300 (± 11 333)
Ce (mg kg^{-1} dry soil) (n = 4)	15.7 (± 3.8)	15.5 (± 3.9)	10.3 (± 1.0)	12.0 (± 2.6)	14.4 (± 2.5)	13.3 (± 3.0)
Zr (mg kg^{-1} dry soil) (n = 4)	30.4 (± 2.7)	22.9 (± 4.1)	22.2 (± 2.6)	23.3 (± 3.8)	33.6 (± 10.8)	39.2 (± 5.9)

higher soil pH than in the control (p = 0.032). Electrical conductivity (EC) of the soil was also affected by the various treatments. The EC of NPK full treated soil was significantly higher than that of the control soil (p = 0.028) or ZSM-5-15 treated soil (p = 0.0057).

No meaningful differences were found between soil NO_3^- or PO_4^{3-} concentrations across treatments, with control soil having an undetectable PO_4^{3-} concentration (Table 2). There was a disparity between the concentrations of NO_3^- and post-incubation NO_3^- under NPK full treatment, indicating that N was nitrified in this treatment only. The full NPK treatment resulted in significantly more mineralised NO_3^- compared to all other treatments (Table S4). C : N ratio varies across treatments, with no statistically significant deviation from the control across treatments for C : N ratio, or C and N content alone. The non-statistically significant differences seen between NO_3^- concentrations differ from the consistent overall N content of the soil due to nitrate making up only a small proportion of total N compounds in the soil.

Comparing the elemental concentrations for macro- and micronutrients across the treatments reflects broadly similar nutrient profiles (Table 2). The only element to have significantly different elemental concentrations was Cu. ZSM-5-15 treated soils had much higher Cu concentrations, with more than 5× the amount of Cu present in soil as compared to the NPK full treated soil (p = 0.007). The Cu content of soil in the BEA-19 treatment was also significantly different to NPK full (p = 0.26). Soil nanomaterial constituent concentrations were uniform across treatments other than for Al. BEA-19 Al soil content was significantly lower than that of the control soil (p = 0.0084).

NPK full treatment produced the greatest N_2O emissions in week 2 (Fig. 1A), but also cumulatively (Fig. S1A). The NPK half combination treatments were consistently low producers of N_2O with one notable exception. Co-addition of ZSM-5-15 NM with NPK half produced 42% more N_2O over the course of the 8 week period as compared to NPK half addition alone. This is most pronounced in week 2, as with the NPK full N_2O emissions. N_2O emissions are significantly different across exposure weeks ($p = 2.58 \times 10^{-10}$). NPK full N_2O emissions are significantly different to all treatments ($p < 0.05$) other than ZSM-5-15 (p = 0.793). ZSM-5-15 produces elevated emissions, producing significantly more N_2O emissions than the control soil (p = 0.0165).

CO_2 evolution was used as a proxy for soil respiration (Fig. 1B), with cumulative CO_2 produced from each treatment also calculated (Fig. S1B). Initially, CO_2 evolution reflects a similar trend to N_2O emissions, with NPK full treatment having the greatest emissions at weeks 1 and 2, as seen in Fig. 1B. Towards the end of the 8 week growing period CO_2 emissions are elevated above week 1 CO_2 emissions, with an associated increase in respiratory activity, from ZSM-5-15, $Ce_{0.75}Zr_{0.25}O_2$ and NPK half treatments. Week of exposure had a significant effect on CO_2 emissions captured ($p = 1.47 \times 10^{-8}$). Control CO_2 emissions were significantly different compared to all other treatments (Table S6), other than NPK full application (p = 0.0785).

Analysis of NH_3 gas emissions was performed for all 8 weeks of growing, however, results greater than the limit of detection were only found for week 1 of the experiment (Fig. 1C). Comparison of NH_3 gas emissions between treatments showed that NPK full and control soil were statistically significantly different (p = 0.0000323). Emission factors of NH_3 and N_2O emissions are available in Fig. S2.

NO_3^- losses in leachate peaked for all treatments at week 4, as shown in Fig. 2A, other than for the ZSM-5-15

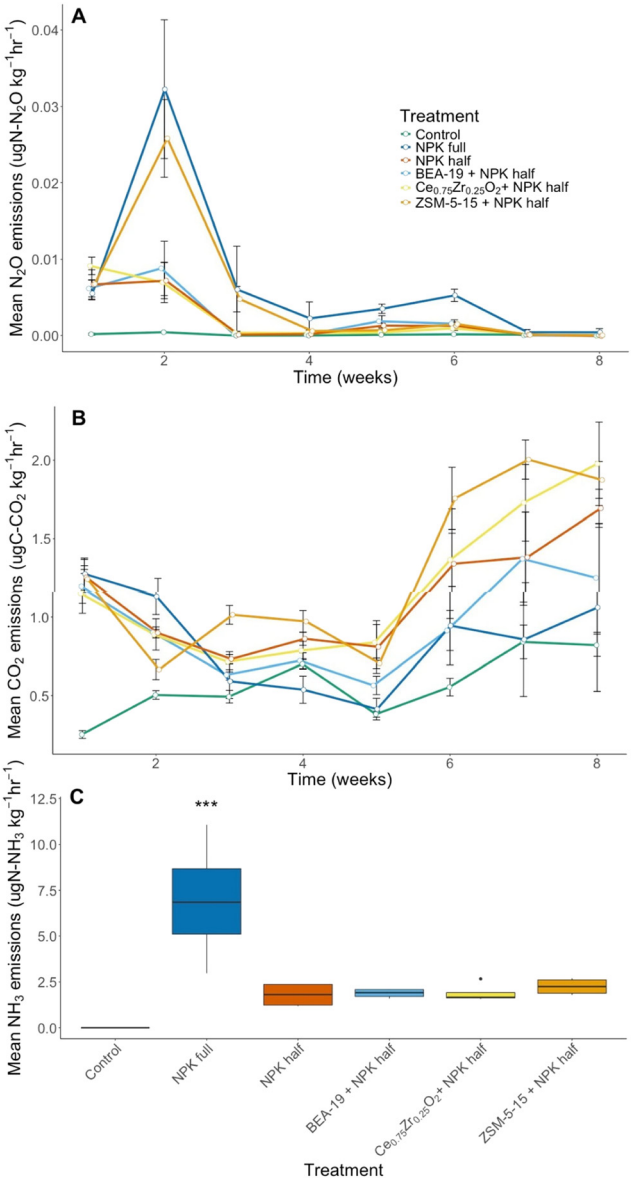

Fig. 1 (A) Weekly time course of soil N_2O emissions across the five different treatments and control. Error bars indicate standard error from the mean (SEM) based on 4 replicates. (B) Weekly time course of soil CO_2 emissions across the five different treatments and control. Error bars indicate SEM of 4 replicates. (C) Soil NH_3 gas emissions in week 1 of the experiment. Error bars indicate SEM from 4 replicates. "***" is used to denote a statistically significant result as compared to the control of $p < 0.0001$.

treated soil, which peaked in week 8 with 12.9 mg L^{-1} of NO_3^- in the leachate. This is not the highest NO_3^- leachate concentration overall, which is found at week 4 in the control soil (16.6 mg L^{-1}). NPK full has the lowest NO_3^- emissions overall. All treatments, other than BEA-19, generated lower NO_3^- leachate concentrations than the control (Table S5). Exposure duration (week) and treatment have a significant effect on the NO_3^- emissions arising from the $Ce_{0.75}Zr_{0.25}O_2$ NM treatment (p = 0.013), with exposure duration (week) also proving significant for NPK half (p = 0.034) and ZSM-5-15 (p = 0.046) treated soil NO_3^- concentrations.

The PO_4^{3-} concentration in the soil was much higher for NPK full than for all the other treatments (0.099 mg L^{-1}), as seen in Fig. 2B. A statistically significant difference was found between the PO_4^{3-} soil concentration of NPK full and control treatments (p = 0.00633). There was a minor reduction in PO_4^{3-} emissions from $Ce_{0.75}Zr_{0.25}O_2$ and ZSM-5-15 treatments relative to the half NPK treatment, this difference, however, was not statistically significant. ZSM-5-15 treatment is significantly correlated with exposure duration (week) (p = 0.0053).

NH_4^+ concentration in leachate peaked in week 1 before rapidly decreasing, with NPK full emissions reducing by 1 mg L^{-1} per week until levels stabilise from week 4 (Fig. 2C). NH_4^+ emissions from the NPK full treated soil are significantly higher than the control across all timepoints ($p = 2.48 \times 10^{-6}$) and are significantly correlated with treatment duration (week) (p = 0.00075), as is evident from Fig. 2C. NPK full treatment NH_4^+ emissions are also significantly different to BEA-19 (p = 0.0036), NPK half (p = 0.0048) and ZSM-5-15 treatment emissions (p = 0.0079). The lack of significant differences between $Ce_{0.75}Zr_{0.25}O_2$ and NPK full treatments is indicative that while the increase in emissions under $Ce_{0.75}Zr_{0.25}O_2$ treatment is not different to the other treatments, it is still elevated.

The highest lettuce yields were produced under $Ce_{0.75}Zr_{0.25}O_2$ (40.8 g) and ZSM-5-15 (43.5 g) treatments, with NPK half treatment alone producing on average 38 g lettuce, as shown in Fig. 3A. Significant increases compared to the control lettuce yield were found under ZSM-5-15 (p = 0.027) and $Ce_{0.75}Zr_{0.25}O_2$ treatment (p = 0.017). Images of the lettuces before harvest at week 8 are provided in Fig. S3.

MDA concentration is a measure of lipid peroxidation, or the effect of ROS on cell membranes. Control lettuce had the lowest MDA concentration of 0.0073 nmol mg^{-1} of lettuce tissue (Fig. 3B). Similarly, NPK half, BEA-19 and $Ce_{0.75}Zr_{0.25}O_2$ treated lettuces didn't show the presence of the stress marker, although variability in the BEA-19 data was large. MDA levels were elevated under NPK full and ZSM-5-15 treatments, but these were not found to be statistically significant increases in MDA concentration relative to the control lettuce.

The micronutrient tissue concentrations, apart from Zn, appear to show similar trends (Fig. 3C). Control tissues have higher concentrations of Cu, Mn and Mg ($p < 0.05$) compared to all other treatments. BEA-19 treated lettuce had a lower yield than controls and it can be seen to have higher micronutrient concentrations of Ca, Cu, Fe, Mn and Mg. There were no statistically significant differences found between treatments for any other micronutrients other than Zn. N content of ZSM-5-15 grown lettuce was significantly greater than that in the control lettuce (p = 0.0067). The P content of NPK full treated lettuce was greater than that in control (p = 0.022), BEA-19 (p = 0.012), or $Ce_{0.75}Zr_{0.25}O_2$ lettuce (p = 0.043). $Ce_{0.75}Zr_{0.25}O_2$ lettuce had significantly lower K content than the control (p =

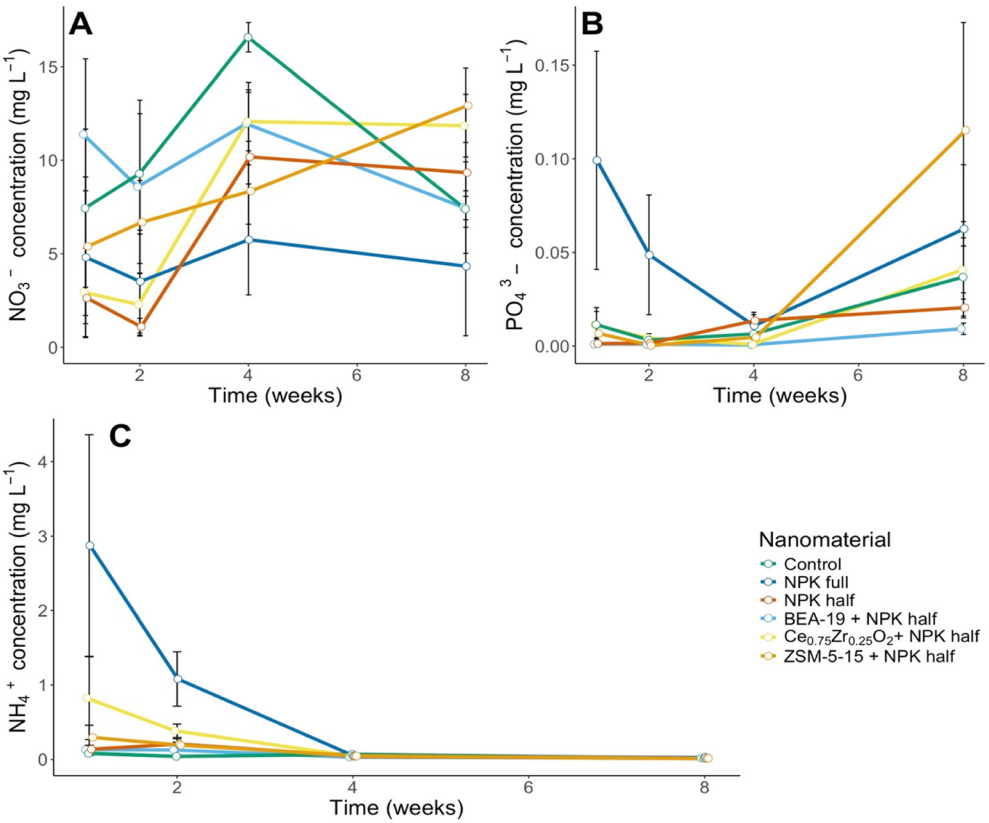

Fig. 2 (A) NO_3^- concentration in leachate emissions recorded at weeks 1, 2, 4, and 8 across the six treatments. (B) PO_4^{3-} concentration in leachate across weeks 1, 2, 4 and 8. (C) NH_4^+ concentration in leachate recorded at weeks 1, 2, 4 and 8. Error bars for A–C reflect SEM based on 4 replicates.

0.038) or NPK full (p = 0.013) lettuce. Differences in elemental concentrations of NM constituent elements in lettuce tissues can be found in Fig. S4.

The Ce fraction of the NM is completely transformed from the original $Ce_{0.75}Zr_{0.25}O_2$ in the soil. The linear combination fit (Fig. 4A) is able to fully describe the transformation of the NM in soil using the X-ray absorption near edge structure (XANES) spectra of CeO_2 (19.6% ± 0.8%) and $Ce_{0.9}Zr_{0.1}O_2$ (80.4% ± 0.8%). The results of the linear combination fit were not able to fully reproduce the Zr K-edge experimental spectra for the $Ce_{0.75}Zr_{0.25}O_2$ treated soil, however the Zr K-edge XANES spectrum for the $Ce_{0.75}Zr_{0.25}O_2$ grown lettuce tissue shows that $Ce_{0.75}Zr_{0.25}O_2$ is translocated into aboveground tissues as well as Zr metal and $ZrCl_4$. Reference standards and experimental spectra are presented in Fig. S5.

4. Discussion

4.1. N_2O emissions and soil respiration are elevated under ZSM-5-15 treatment

ZSM-5-15 treatment both elevates N_2O emissions and increases the soil respiration rate. The observed peak in N_2O emissions at week-2 is due to a lag in microbial gas production after the immediate addition of nutrients. N was added to soil in the form of urea which is hydrolysed to NH_4^+ *via* the enzyme urease, which is then utilised in nitrification, producing N_2O. Nitrate can also be denitrified into N_2O in addition to nitrification as a source of N_2O. Zeolite application has been shown to increase the abundance of ammonia-oxidising archaea and to increase ammonia monooxygenase enzyme activity in agricultural waste.[40] ZSM-5-15 may therefore be impacting nitrifying microbes and elevating N_2O emissions either through increasing nitrifying community size, or directly impacting on enzymatic activity. Soil pH was reduced under the NPK full treatment due to the increased addition of N fertiliser triggering subsequent nitrification, producing H^+ ions, as seen in eqn (1), which shows the *Nitrosomonas* catalysed reduction of NH_4^+ in soil. This correlates with the reduction in NH_3 gas emissions and NH_4^+ in the leachate. However, there is no reduction in soil pH under the ZSM-5-15 treatment. If the theorised mechanism is that ZSM-5-15 is able to upregulate nitrification, then, as with the NPK full treatment, there should be a corresponding drop in soil pH. The absence of a pH change may mean that ZSM-5-15 has a buffering capacity, potentially through its extra-framework ion (NH_4^+) being released, leaving binding sites for H^+ ions through a process of ion exchange.[41,42] Extra-framework ions are held in the pore spaces of the zeolites' 3D structure and are not chemically bound to the NM, allowing greater capacity for ion exchange than other comparable minerals.[43]

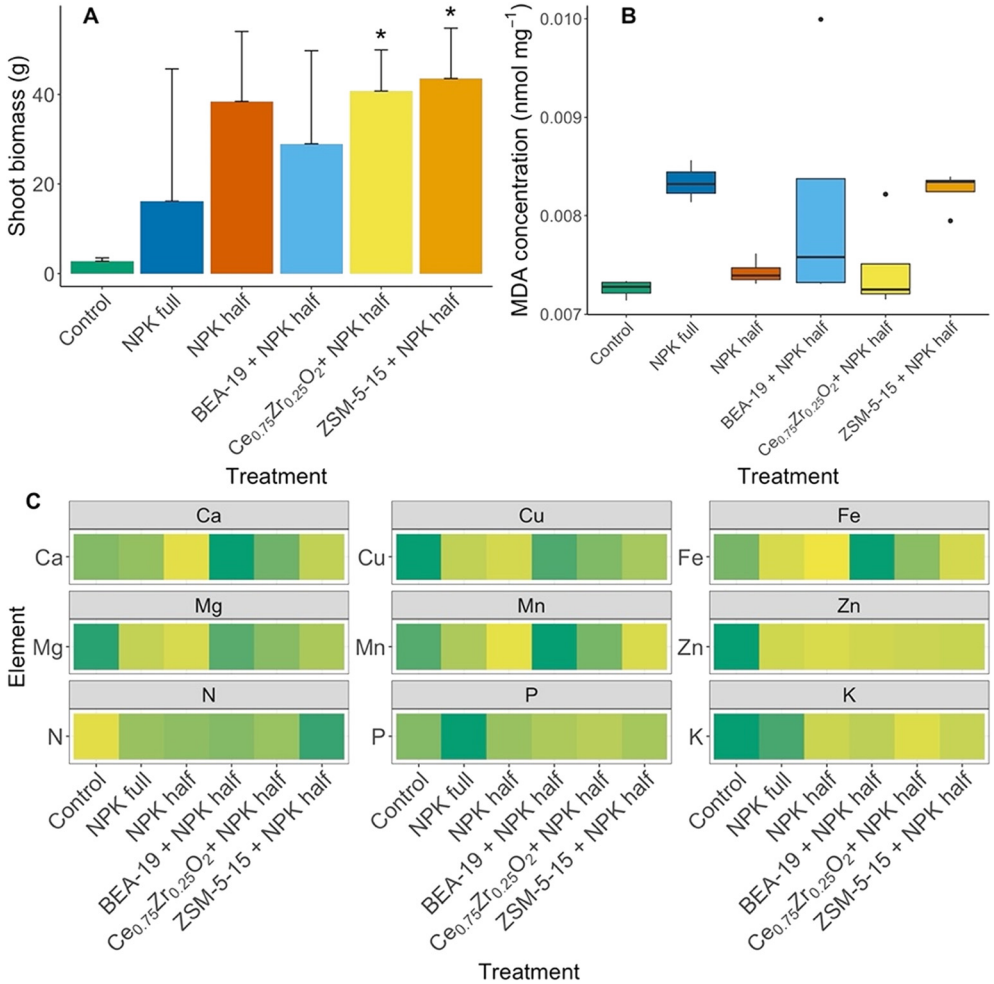

Fig. 3 A) Lettuce aboveground biomass after destructive sampling at week 8. Error bars indicate standard deviation (n = 4). Significantly different means compared to the control are denoted using '*' where $p < 0.05$. B) Malondialdehyde (MDA) concentration in lettuce shoot tissue including mean and SEM (n = 4). Black dots signify outliers. C) Relative concentration of macro- and micronutrient elements of interest in lettuce tissue compared across the six treatments (n = 4), numerical element concentration data is available in Table S7. N content was determined *via* elemental analysis, all other nutrients were determined *via* ICP-OES.

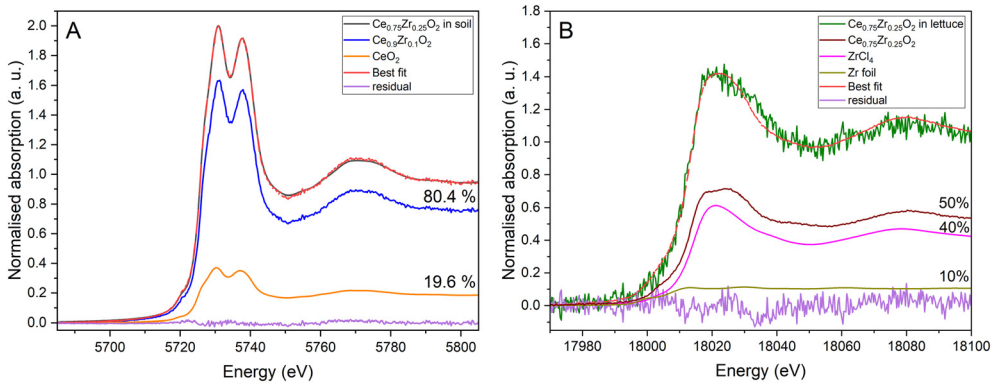

Fig. 4 (A) Ce L_3-edge normalised XANES spectrum of $Ce_{0.75}Zr_{0.25}O_2$ treated soil samples and best linear combination fit of XANES profiles of $Ce_{0.9}Zr_{0.1}O_2$ and CeO_2. (B) Zr K-edge normalised XANES spectrum of $Ce_{0.75}Zr_{0.25}O_2$ grown lettuce tissue and best linear combination fit of XANES profiles of pristine $Ce_{0.75}Zr_{0.25}O_2$ and $ZrCl_4$ and Zr metal foil.

$$2NH_4^+ + 4O_2 + 4e^- \rightarrow 2NO_3 + 4H^+ + 2H_2O + 12e^- \quad (1)$$

Alternatively, the ZSM-5-15 triggered N_2O emissions could be through an effect on the final stage of denitrification. This

might be through ZSM-5-15 having a toxic effect on soil microbes that are responsible for reducing N_2O to N_2, causing there to be a proportional increase of N_2O. Nitrous oxide reductase (NOS) is the only enzyme found to reduce N_2O to N_2 in the N cycle.[44] It may be that ZSM-5-15 has an inhibitory effect on this enzyme, producing elevated N_2O emissions, however, this theory doesn't align with the soil respiration data or the leachate emissions data.

The increase in soil respiration, as determined *via* CO_2 production, cannot definitively be determined to be produced through either an increase in lettuce root biomass, impacts on the soil microbial community, or both. Previous research shows that the metabolic quotient of soil increased under zeolite application although no impact on respiratory activity was seen.[45] Due to the sampling procedure utilised, no accurate data for root biomass was found in this study, leaving the mechanism unclear.

ZSM-5-15, nor either of the other NM treatments produced any impact on NH_3 emissions, with the highest emissions being from NPK full application. Zeolite addition to poultry manure has been shown to reduce NH_3 volatilisation by up to 44%.[46] While the organic matter content of manure is much higher than that of soil, the ability to reduce emissions is relevant. The low NH_3 emissions may be due to the rate of nitrification in the ZSM-5-15 treated soil, whereby NH_3 is being converted rather than emitted as a gas.

Rather than promoting microbial community shifts, ZSM-5-15 may have nanozyme activity and could be directly involved in conversion of NH_4^+ to N_2O. Other zeolite nanozymes have been developed previously, but were functionalised with Zn.[47,48] As ZSM-5-15 has no transition metal functionalisation, these findings are indicative that ZSM-5-15 is able to produce a shift in typical terrestrial N cycling, as compared to control or NPK half treatment alone, likely by promoting nitrifying microbe abundance or enzymatic activity.

4.2. Leaching loss dynamics over time and with NM treatment

The timing and magnitude of nutrient emissions in leachate is consistent with the gas emissions data for ZSM-5-15 treatment and its effect on nitrification sourced N_2O emissions. In week 1, the lowest NO_3^- concentration in the leachate was for $Ce_{0.75}Zr_{0.25}O_2$ treatment, whilst NO_3^- concentrations were highest in the control soil. An explanation for this could be due to the NPK half addition producing a lag in emissions as seen with N_2O, due to urea's conversion by urease to NH_4^+ before conversion to NO_3^-. The peak in ammonium concentration in week 1, and decline by week 4, coincides with the peak in nitrate emissions in leachate. The control soil had the lowest N_2O emissions, as compared to the NPK full and all NM with half NPK treatments. This could be due to nitrification of NH_4^+ to NO_3^- occurring more completely, with reduced nitrifier sources of N_2O. Both zeolites used in this experiment had NH_4^+ as their extra-framework ions. This binding capacity for NH_4^+ means that there may be a delay in nitrification under this treatment due to slow release of the NH_4^+. Overall, this will lower the amount of nitrification in the soil at later stages due to the binding of NH_4^+. The increase in leachate concentration of NO_3^- over time for the zeolites indicates a slow release of these extra-framework ions, with BEA-19 potentially having a stronger affinity for NH_4^+ than ZSM-5-15. BEA and ZSM-5 type zeolites have been compared for ion exchange application in catalytic converter exhaust gas adsorption, reflecting the fact that both have catalytic and adsorptive effects across applications.[49] This also has a further impact on denitrification, due to low nitrification later in the growth period limiting the supply of NO_3^- to denitrifying microbes.

NO_3^- leachate emissions are highest for the control group, peaking in week 4, this is partnered with the lowest rate of CO_2 evolution, indicating that denitrification is stunted in the control soils through a lack of soil microbial activity. This reduced microbial activity, combined with the lack of NPK input to the soil, causes the low N_2O emissions. The NO_3^- emissions for NPK full treatment are likely so low due to the soil pH reduction impacting on soil microbial activity, as displayed through the reduced CO_2 emissions data. This lack of activity slows the N cycle, with reduced NH_4^+ and NO_3^- emissions. NPK half and $Ce_{0.75}Zr_{0.25}O_2$ treatments follow the same trend for NO_3^- emissions; $Ce_{0.75}Zr_{0.25}O_2$ produces slightly elevated emissions but this is coupled with greater soil respiration. NO_3^- emissions for ZSM-5-15 are unique, peaking in week 8, reflecting the time period needed for conversion of NH_4^+ to NO_3^-, further indicating that the earlier (week 2) N_2O emissions peak is nitrification sourced rather than arising from denitrification.

Leachate losses over time reflect changing adsorption dynamics and local conditions for the NMs, with the highest PO_4^{3-} emissions occurring in ZSM-5-15 treated soil at week 8. ZSM-5-15 is negatively charged and so, unlike $Ce_{0.75}Zr_{0.25}O_2$, there are no binding dynamics between it and PO_4^{3-}, thus increasing PO_4^{3-} emissions. BEA-19 however has an even more negative zeta potential. Zeolites have previously been utilised for simultaneous removal of NH_4^+ and PO_4^{3-} in water purification, using Ca^{2+} ions to remove PO_4^{3-}.[50] As the extra-framework ion, NH_4^+, is slowly released over time, pore spaces in the structure of the zeolite will become available, permitting ion exchange. This may happen with H^+ ions as mentioned previously but also other cations, for example Ca^{2+}, K^+ and Na^+. As ion exchange continues to occur this may result in formation of $Ca_3(PO_4)_2$, minimising PO_4^{3-} leaching under BEA-19 treatment. While both BEA-19 and ZSM-5-15 are negatively charged nano-zeolites with relatively similar Si : Al ratios (19 and 15, respectively), pore sizes (6.8 Å and 5.5 Å) and primary particle sizes, they have very different impacts on gaseous and leachate emissions, and final soil concentrations of NO_3^- and PO_4^{3-}, however the physical basis for these differences is currently unknown.

The leachate emissions data, combined with the N_2O and CO_2 emissions in particular, have a shared narrative around

the impact of ZSM-5-15 NMs on soil nitrification. Differences between the NMs, both in terms of constituent elements and hydrodynamic size, zeta potential and other properties, are likely significant in understanding the mechanisms that impact their leachate emissions.

4.3. NM zeta potential, ion exchange capacity, and transformations within the soil matrix, influence NM–soil component interactions

Comparing SEM/TEM derived particle sizes and water-dispersed hydrodynamic sizes it is clear that the NMs exist as aggregates under the exposure conditions. Further agglomeration and transformation will then have altered the NMs before interaction with plant roots, altering their capacity for translocation into other plant tissues. The XANES data reflects that the NMs are undergoing transformations within the soil environment. Ce and Zr were below the limit of detection for ICP-OES in lettuce tissue, while this has meant a high quality XANES spectra was not able to be generated for Ce, indicating limited bioaccumulation. In order to understand if the small amounts of translocated NMs undergo further transformations in plant tissues, studies at higher, less environmentally realistic, concentrations are required. The LCF for Ce L3-edge XANES spectra of $Ce_{0.75}Zr_{0.25}O_2$ in soil clearly shows Zr^{4+} ions may leach from the mixed metal oxide, leaving $Ce_{0.9}Zr_{0.1}O_2$ and CeO_2 in the soil. Previous study shows that CeO_2 has limited effect on soil microbial biomass, however there may be uptake of Ce by soil microbes.[51] This indicates one of the ways in which CeO_2 can interact with the biotic components of soil. $Ce_{0.75}Zr_{0.25}O_2$, $ZrCl_4$ and Zr metal were the primary forms of Zr found in the lettuce samples after the 8 weeks of incubation. Whether the leached Zr^{4+} ions are forming $ZrCl_4$ in the soil or inside the plant roots/shoots is unclear due to low quality soil spectra. $ZrCl_4$ is used industrially and as a catalyst, however ZrO_2 is the more popular nano-form for application. $ZrCl_4$ is not a particularly stable form of Zr and reacts with water indicating that this is perhaps a transient Zr form.

Of the NM properties, zeta potential and in turn, ion exchange capacity, play the most significant role in NM–soil interactions. Clay and organic matter are negatively charged so the positively charged $Ce_{0.75}Zr_{0.25}O_2$ is likely to have been held in the soil matrix, potentially forming interactions with PO_4^{3-} and NO_3^-. This could form part of its mechanism, improving lettuce biomass through slow release of essential nutrients like PO_4^{3-} and NO_3^-, without increasing N emissions. This is particularly relevant post transformation, as CeO_2 has been shown to heteroaggregate with soil clay particles and other natural soil colloids.[52] There is a lack of $CePO_4$ seen in the experimental soil samples, which indicates that any CeO_2–PO_4^{3-} interaction would be through weaker forces such as van der Waal forces in larger agglomerates rather than *via* chemical bonding. Positively charged NMs also interact differently with plant roots than negatively charged ones, typically remaining on the outside of root surfaces.[5,53,54] CeO_2 NMs surface charge can be modulated through application of PO_4^{3-} ions, acting to neutralise and change the zeta potential of the NMs, encouraging translocation into aboveground plant tissues.[55,56] The negatively charged ZSM-5-15 is capable of forming interactions with soil cations, using ion exchange to prevent soil pH reduction while promoting nitrification through release of NH_4^+. The binding dynamics between ZSM-5-15 and BEA-19 are clearly different, despite the similarities in their compositions, Si/Al ratio, zeta potential and agglomerate size. Both zeolites are bound to NH_4^+ and have similar pore sizes, of 6.8 and 5.5 Å for BEA-19 and ZSM-5-15, respectively. With two zeolites of such great similarity, it is hard to determine how they have such different effects on soil N cycling, leachate emissions and lettuce growth on the basis of this dataset alone.

4.4. $Ce_{0.75}Zr_{0.25}O_2$ and ZSM-5-15 positively impact lettuce growth with maintained crop quality

ZSM-5-15 is able to increase both lettuce biomass and N content, however the impact of ZSM-5-15 on N_2O emissions means that it cannot be considered as a sustainable alternative to conventional fertilisation. BEA-19 improves the micronutrient status of lettuce but has a negative impact on lettuce biomass accumulation. This is suggested to be due to the very low lettuce growth seen under BEA-19 treatment, which may be the result of a deficiency in Zn.[57] The Zn concentration is much higher in the control lettuce, with the other treatments producing lettuces all within a similar range for Zn concentration in shoot tissue (0.00011–0.00021 mg g^{-1}). Control lettuce biomass was much lower than all other treatments, indicating that the control lettuces' stunted growth was due to a lack of available nitrogen and phosphate in particular, which led to a greater but still deficient Zn concentration.[58] NPK full treatment acidified the soil; this resulting change in soil pH is the most probable cause of the decreased biomass accumulation, with the NPK half treatment having a similar soil pH at week 8 to the control treatments, with resulting greater lettuce biomass accumulation than in the NPK full treatment. $Ce_{0.75}Zr_{0.25}O_2$ treatment promotes lettuce biomass accumulation, without impacting on soil N emissions. However, the NM fails to improve the crop's quality, with no significant differences to any other treatments for macro- or micronutrient tissue concentrations. Therefore, the ratio of nutrients to biomass remains consistent and there is greater lettuce biomass under NM treatments, leading to maintenance of lettuce's quality in terms of nutritive content, partnered with improved yield. Under alkaline conditions, as in all treatments other than NPK full, the increased N content of soil is linked to increased Zn, Cu, Fe and Mn uptake. However, increased P fertiliser additions may have a negative effect on micronutrient uptake, having been shown to affect Zn among others.[59]

None of the lettuce tissues measured displayed high MDA content, a key marker of lipid peroxidation in response to reactive oxygen species production during oxidative stress. MDA concentration was only recorded after

destructive sampling so transient changes in MDA concentration over the plants' growing period were not studied. Slightly elevated MDA concentrations were found for NPK full and ZSM-5-15 grown lettuce. This may be due to the more acidic soil found under NPK full treatment, while the effect of ZSM-5-15 on lettuce MDA levels may be due to the action of the NM itself, *i.e.*, a physical effect. It could be through this minor stress that greater biomass accumulation was seen, as many nanofertilisers act to improve crop growth through initiation of minor stress, triggering improved crop stress tolerance through prior activation of stress signalling pathways.[60]

Nano-CeO_2 has been shown to have an antioxidative effect, mimicking the antioxidative enzymes catalase (CAT) and superoxide dismutase (SOD) until binding with phosphate.[61,62] From the Ce L3-edge XANES spectra linear combination fitting it is clear that there is very limited binding of Ce to PO_4^{3-} in the soil environment, indicating that there is potential for CeO_2 to be acting as a nanozyme, promoting lettuce growth and improving crop stress resilience. However, how the heteroagglomerates of CeO_2 with associated soil anions, clay particles and colloids behave, and how these other compounds are able to influence nanozyme activity is currently unknown.

4.5. Outlook

ZSM-5-15 treatment drives changes in the soil N cycling, most notably through increasing N_2O emissions. This is theorised to be through the action of ZSM-5-15 NMs on nitrifying microbes, likely be aided through its supplementation of NH_4^+ ions as part of its structure. This theory is supported by the soil respiration and leachate nutrient emissions data, in particular NH_4^+ and NO_3^- emissions. Disentangling the mechanism of ZSM-5-15 action on N_2O emissions requires further study. Stable isotope ^{15}N labelling of NO_3^- and NH_4^+ would be required to determine whether N_2O is being produced *via* nitrification or denitrification pathways. If the increase in N_2O from ZSM-5-15 is through nitrification then qPCR analysis of relevant N-cycling genes in bacteria, but also archaeal and fungal groups, would elucidate how ZSM-5-15 may be affecting the soil microbial community. Further research on shifts in microbial communities upon NM application in conjunction with fertilisers would also aid understanding of potential ecotoxicological impacts of the NMs on soil microbes. Additionally, deciphering what zeolite characteristics trigger the effect would enable improved design and agricultural application of other zeolites also. There are undetermined factors that also influence the differences in NM effect, for example the most significant differences between BEA-19 and ZSM-5-15 zeolite NMs remains unclear in terms of their effect on crop growth and soil N cycling dynamics.

$Ce_{0.75}Zr_{0.25}O_2$ NMs provide a promising avenue for future research, with increased biomass accumulation without triggering increased gaseous or leachate emissions, or soil acidification, whilst also maintaining the lettuce's micronutrient content with this increased biomass accumulation. The mixed metal oxide is likely leaching Zr^{4+} ions, leading to the formation of $ZrCl_4$, $Ce_{0.9}Zr_{0.1}O_2$ and CeO_2, which then act independently in the soil and on the plant. The NMs' zeta potential, particularly relating to ion exchange capacity, interaction with soil colloids, anions and cations, are all important factors in NM activity in soils. The impact of the leached Zr^{4+} ions on soil microorganisms is highly dependent on what compounds it subsequently forms, with $ZrCl_4$ previously shown to impact the reproduction of model terrestrial species *Enchytraeus crypticus*.[63] As such, further research is required to fully determine the broader ecological impacts of $Ce_{0.75}Zr_{0.25}O_2$ NMs release into agroecosystems, especially the extent to which NM transformation products impact different soil species.

NMs transform as they enter the soil, with further transformations inside plant tissues.[64] Understanding how the transformed NMs go on to interact with plant roots and if further transformations occur at the plant root surface due to root exudates or inside plant tissues is yet to be understood for $Ce_{0.75}Zr_{0.25}O_2$, ZSM-5-15 and BEA-19. Just as these NMs are transforming, understanding how these changes alter their agglomeration and binding dynamics is important to reveal how they behave in natural systems. For example, visualising heteroagglomerates would aid in developing more detailed knowledge around NM kinetics, realistic agglomerate size and interactions with biotic soil components. NM heteroaggregates have been studied under lab conditions using scanning transmission electron microscopy (STEM), but methods for complex environmental sample heteroagglomerates and compound identification is lacking.[65–67] To understand how Zr compounds and CeO_2 act in the soil post transformation from $Ce_{0.75}Zr_{0.25}O_2$, these visualisations or other characterisation methods in complex samples are required.

Author contributions

Jessica Chadwick: writing – original draft, investigation, formal analysis, visualisation, conceptualization, funding acquisition. Aleksandar Radu: resources, writing – review and editing. Iuliia Mikulska: formal analysis, visualisation, funding acquisition, writing – review and editing. Swaroop Chakraborty: investigation, funding acquisition, writing – review and editing. Peng Zhang: supervision, funding acquisition. Sami Ullah: conceptualization, supervision, writing – review and editing, funding acquisition. Iseult Lynch: conceptualization, supervision, writing – review and editing, funding acquisition.

Conflicts of interest

There are no conflicts to declare.

Data availability

Supplementary information (SI): statistical test results, lettuce nutrient concentrations and XANES spectra of experimental samples and reference standards. See DOI: **https://doi.org/10.1039/D5EN00526D**.

The data supporting this article have been included as part of the SI.

Acknowledgements

This work was supported by the Biotechnology and Biological Sciences Research Council (BBSRC) and University of Birmingham funded Midlands Integrative Biosciences Training Partnership (MIBTP) grant number BB/T00746X/1. Assistance with figures was provided by Chantal Jackson (University of Birmingham, UK). Gas chromatography and lettuce elemental analysis was undertaken by Fotis Sgouridis (University of Bristol, UK). Soil elemental analysis was performed at the Analytical Facility, Department of Chemistry (University of Birmingham, UK). ICP-OES assistance was provided by Chris Stark (University of Birmingham, UK). Cerium-zirconium oxide nanomaterials were obtained from Promethean Particles *via* the EU-funded NanoSolveIT project (Grant Agreement N° 814572). This work was carried out with the support of Diamond Light Source, instruments B18 for XAS experiments (experiment numbers SP34510-1 and SP39677-1) awarded to Swaroop Chakraborty, Iseult Lynch, Iuliia Mikulska, and Jessica Chadwick and provided *via* the University of Birmingham and Diamond Light Source collaboration. Swaroop Chakraborty acknowledges NERC Independent Research Fellowship (Grant number- *NE/B000187/1*) to support Jessica Chadwick with B18 XAS work at Diamond Light Source for this project.

References

1 J. N. Galloway and E. B. Cowling, Reactive Nitrogen and The World: 200 Years of Change, *Ambio*, 2002, **31**(2), 64–71.
2 V. Smil, *Enriching the Earth: Fritz Haber, Carl Bosch, and the Transformation of World Food Production [Internet]*, The MIT Press, 2000, available from: **https://direct.mit.edu/books/book/2775/Enriching-the-EarthFritz-Haber-Carl-Bosch-and-the**.
3 IPCC, 2023: *Climate Change 2023: Synthesis Report, Contribution of Working Groups I, II and III to the Sixth Assessment Report of the Intergovernmental Panel on Climate Change*, ed. Core Writing Team, H. Lee and J. Romero, IPCC, Geneva, Switzerland, [Internet], 2023, [cited 2024 Jun 3], pp. 35–115, DOI: **10.59327/IPCC/AR6-9789291691647**.
4 L. Wang, C. Hu and L. Shao, The antimicrobial activity of nanoparticles: present situation and prospects for the future, *Int. J. Nanomed.*, 2017, **12**, 1227–1249.
5 E. Spielman-Sun, E. Lombi, E. Donner, D. Howard, J. M. Unrine and G. V. Lowry, Impact of Surface Charge on Cerium Oxide Nanoparticle Uptake and Translocation by Wheat (Triticum aestivum), *Environ. Sci. Technol.*, 2017, **51**(13), 7361–7368.
6 M. Rizwan, S. Ali, M. F. Qayyum, Y. S. Ok, M. Adrees and M. Ibrahim, *et al.*, Effect of metal and metal oxide nanoparticles on growth and physiology of globally important food crops: A critical review, *J. Hazard. Mater.*, 2017, **322**, 2–16.
7 C. Svendsen, L. A. Walker, M. Matzke, E. Lahive, S. Harrison and A. Crossley, *et al.*, Key principles and operational practices for improved nanotechnology environmental exposure assessment, *Nat. Nanotechnol.*, 2020, **15**(9), 731–742.
8 A. Avellan, M. Simonin, E. McGivney, N. Bossa, E. Spielman-Sun and J. D. Rocca, *et al.*, Gold nanoparticle biodissolution by a freshwater macrophyte and its associated microbiome, *Nat. Nanotechnol.*, 2018, **13**(11), 1072–1077.
9 L. Pagano, R. Rossi, J. C. White, N. Marmiroli and M. Marmiroli, Nanomaterials biotransformation: In planta mechanisms of action, *Environ. Pollut.*, 2023, **318**, 120834.
10 G. Zhu, P. Zhang, W. Zhao, N. Shakoor, Y. Sun, Q. Wang, Q. Wang, M. Li, Y. Jiang, Z. Tan, Y. Rui and I. Lynch, Toxicity of metal-based nanomaterials in different organisms, *Toxin Rev.*, 2024, **43**(2), 236–254.
11 C. Xu, C. Peng, L. Sun, S. Zhang, H. Huang and Y. Chen, *et al.*, Distinctive effects of TiO2 and CuO nanoparticles on soil microbes and their community structures in flooded paddy soil, *Soil Biol. Biochem.*, 2015, **86**, 24–33.
12 H. Li, Y. Guo, A. Liang, X. Xu, Y. Hao and H. Shang, *et al.*, Commonly Used Engineered Nanomaterials Improve Soil Health via Suppressing Soil-Borne Fusarium and Positively Altering Soil Microbiome, *ACS EST Eng.*, 2024, **4**(4), 915–927.
13 T. Mudalige, H. Qu, D. Van Haute, S. M. Ansar, A. Paredes and T. Ingle, in *Nanomaterials for Food Applications [Internet]*, ed. A. López Rubio, M. J. Fabra Rovira, M. Martínez Sanz and L. G. Gómez-Mascaraque, Elsevier, 2019, ch. 11 - Characterization of Nanomaterials: Tools and Challenges, pp. 313–353, (Micro and Nano Technologies), available from: **https://www.sciencedirect.com/science/article/pii/B9780128141304000117**.
14 A. Ditta and M. Arshad, Applications and perspectives of using nanomaterials for sustainable plant nutrition, *Nanotechnol. Rev.*, 2016, **5**(2), 209–229.
15 M. Simonin, A. A. M. Cantarel, A. Crouzet, J. Gervaix, J. M. F. Martins and A. Richaume, Negative Effects of Copper Oxide Nanoparticles on Carbon and Nitrogen Cycle Microbial Activities in Contrasting Agricultural Soils and in Presence of Plants, *Front. Microbiol.*, 2018, **9**, 3102.
16 B. M. Abu-Zied, W. Schwieger and A. Unger, Nitrous oxide decomposition over transition metal exchanged ZSM-5 zeolites prepared by the solid-state ion-exchange method, *Appl. Catal., B*, 2008, **84**(1), 277–288.
17 B. P. Narasaiah, S. Koppala, P. Kar, B. Lokesh and B. K. Mandal, Photocatalytic and Antioxidant Studies of Bioinspired ZrO2 Nanoparticles Using Agriculture Waste Durva Grass Aqueous Extracts, *J. Hazard. Mater. Adv.*, 2022, **7**, 100112.
18 X. Gui, Z. Zhang, S. Liu, Y. Ma, P. Zhang and X. He, *et al.*, Fate and Phytotoxicity of CeO2 Nanoparticles on Lettuce

Cultured in the Potting Soil Environment, *PLoS One*, 2015, **10**(8), e0134261.

19 Z. Zhang, X. He, H. Zhang, Y. Ma, P. Zhang and Y. Ding, *et al.*, Uptake and distribution of ceria nanoparticles in cucumber plants, *Metallomics*, 2011, **3**(8), 816–822.

20 E. S. Rodrigues, G. S. Montanha, E. de Almeida, H. Fantucci, R. M. Santos and H. W. P. de Carvalho, Effect of nano cerium oxide on soybean (*Glycine max* L. Merrill) crop exposed to environmentally relevant concentrations, *Chemosphere*, 2021, **273**, 128492.

21 W. J. Stark, M. Maciejewski, L. Mädler, S. E. Pratsinis and A. Baiker, Flame-made nanocrystalline ceria/zirconia: structural properties and dynamic oxygen exchange capacity, *J. Catal.*, 2003, **220**(1), 35–43.

22 Y. Zheng, Z. Hu, H. Huang, W. Ji, M. Sun and C. Chen, Synthesis and Characterization of Nanometer $Ce_{0.75}Zr_{0.25}O_2$ Powders by Solid-State Chemical Reaction Method, *J. Nanomater.*, 2011, **2011**, 1–7.

23 D. Jiang, D. Ni, Z. T. Rosenkrans, P. Huang, X. Yan and W. Cai, Nanozyme: new horizons for responsive biomedical applications, *Chem. Soc. Rev.*, 2019, **48**(14), 3683–3704.

24 M. Jendrlin, A. Radu, V. Zholobenko and D. Kirsanov, Performance modelling of zeolite-based potentiometric sensors, *Sens. Actuators, B*, 2022, **356**, 131343.

25 W. Song, R. E. Justice, C. A. Jones, V. H. Grassian and S. C. Larsen, Synthesis, Characterization, and Adsorption Properties of Nanocrystalline ZSM-5, *Langmuir*, 2004, **20**(19), 8301–8306.

26 S. R. Dhage, S. P. Gaikwad, P. Muthukumar and V. Ravi, Synthesis of Ce0.75Zr0.25O2 at 100 °C, *Ceram. Int.*, 2005, **31**(1), 211–213.

27 G. A. Achari and M. Kowshik, Recent Developments on Nanotechnology in Agriculture: Plant Mineral Nutrition, Health, and Interactions with Soil Microflora, *J. Agric. Food Chem.*, 2018, **66**(33), 8647–8661.

28 *Nutrient Management Guide RB209 Section 6 Vegetables and bulbs.pdf*, AHDB, 2017.

29 S. A. Comer-Warner, S. Ullah, A. Dey, C. L. Stagg, T. Elsey-Quirk and C. M. Swarzenski, *et al.*, Elevated temperature and nutrients lead to increased N2O emissions from salt marsh soils from cold and warm climates, *Biogeochemistry*, 2024, **167**(1), 21–37.

30 F. Sgouridis and S. Ullah, Soil Greenhouse Gas Fluxes, Environmental Controls, and the Partitioning of N2O Sources in UK Natural and Seminatural Land Use Types, *J. Geophys. Res.: Biogeosci.*, 2017, **122**(10), 2617–2633.

31 R. L. Mulvaney, Nitrogen—Inorganic Forms, in *Methods of Soil Analysis [Internet]*, John Wiley & Sons, Ltd, 1996, pp. 1123–1184, available from: **https://onlinelibrary.wiley.com/doi/abs/10.2136/sssabookser5.3.c38**.

32 K. M. Miranda, M. G. Espey and D. A. Wink, A Rapid, Simple Spectrophotometric Method for Simultaneous Detection of Nitrate and Nitrite, *Nitric Oxide*, 2001, **5**(1), 62–71.

33 J. Murphy and J. P. Riley, A modified single solution method for the determination of phosphate in natural waters, *Anal. Chim. Acta*, 1962, **27**, 31–36.

34 CEM, *Mars 6 Microwave Acid Digestion Method Note Compendium*, 2019.

35 S. Diaz-Moreno, M. Amboage, M. Basham, R. Boada, N. E. Bricknell and G. Cibin, *et al.*, The Spectroscopy Village at Diamond Light Source, *J. Synchrotron Radiat.*, 2018, **25**(Pt 4), 998–1009.

36 A. J. Dent, G. Cibin, S. Ramos, S. A. Parry, D. Gianolio and A. D. Smith, *et al.*, Performance of B18, the Core EXAFS Bending Magnet beamline at Diamond, *J. Phys.: Conf. Ser.*, 2013, **430**, 012023.

37 G. Dennis, W. Helsby, D. Omar, I. Horswell, N. Tartoni and S. Hayama, *et al.*, First results using the new DLS Xspress4 digital pulse processor with monolithic segmented HPGe detectors on XAS beamlines, *AIP Conf. Proc.*, 2019, **2054**(1), 060065.

38 B. Ravel and M. Newville, ATHENA, ARTEMIS, HEPHAESTUS: data analysis for X-ray absorption spectroscopy using IFEFFIT, *J. Synchrotron Radiat.*, 2005, **12**(4), 537–541.

39 R Core Team, *R: A language and environment for statistical computing, v4.0.2*, R Foundation for Statistical Computing, Vienna, Austria, 2023.

40 X. Wu, L. Ren, J. Zhang and H. Peng, Effects of Zeolite and Biochar Addition on Ammonia-Oxidizing Bacteria and Ammonia-Oxidizing Archaea Communities during Agricultural Waste Composting, *Sustainability*, 2020, **12**(16), 6336.

41 O. H. Ahmed, G. Sumalatha and A. M. N. Muhamad, *Use of zeolite in maize (Zea mays) cultivation on nitrogen, potassium and phosphorus uptake and use efficiency*, 2010.

42 H. Leinonen and J. Lehto, Purification of metal finishing waste waters with zeolites and activated carbons, *Waste Manag. Res. J. A Sustain. Circ. Econ.*, 2001, **19**(1), 45–57.

43 M. Oguz and H. Arslan, Enhancing soil health with increasing the nitrogen content of zeolite-based fertilizers for agricultural applications, *Int. J. Environ. Health Res.*, 2025, **16**, 1–17.

44 M. M. M. Kuypers, H. K. Marchant and B. Kartal, The microbial nitrogen-cycling network, *Nat. Rev. Microbiol.*, 2018, **16**(5), 263–276.

45 G. Mühlbachová and T. Šimon, Effects of zeolite amendment on microbial biomass and respiratory activity in heavy metal contaminated soils, *Plant, Soil Environ.*, 2003, **49**(12), 536–541.

46 M. Kithome, J. W. Paul and A. A. Bomke, Reducing Nitrogen Losses during Simulated Composting of Poultry Manure using Adsorbents or Chemical Amendments, *J. Environ. Qual.*, 1999, **28**(1), 194–201.

47 C. Chen, Z. Hu, J. Ren, S. Zhang, Z. Wang and Z. Y. Yuan, ZnO Nanoclusters Supported on Dealuminated Zeolite β as a Novel Catalyst for Direct Dehydrogenation of Propane to Propylene, *ChemCatChem*, 2019, **11**(2), 868–877.

48 T. Fu, C. Xu, R. Guo, C. Lin, Y. Huang and Y. Tang, *et al.*, Zeolitic Imidazolate Framework-90 Nanoparticles as Nanozymes to Mimic Organophosphorus Hydrolase, *ACS Appl. Nano Mater.*, 2021, **4**(4), 3345–3350.

49 T. J. Toops, A. J. Binder, P. Kunal, E. A. Kyriakidou and J. S. Choi, Analysis of Ion-Exchanged ZSM-5, BEA, and SSZ-13 Zeolite Trapping Materials under Realistic Exhaust Conditions, *Catalysts*, 2021, **11**(4), 449.

50 N. Karapınar, Application of natural zeolite for phosphorus and ammonium removal from aqueous solutions, *J. Hazard. Mater.*, 2009, **170**(2), 1186–1191.

51 L. Vittori Antisari, S. Carbone, A. Gatti, G. Vianello and P. Nannipieri, Toxicity of metal oxide (CeO2, Fe3O4, SnO2) engineered nanoparticles on soil microbial biomass and their distribution in soil, *Soil Biol. Biochem.*, 2013, **60**, 87–94.

52 G. Cornelis, B. Ryan, M. J. McLaughlin, J. K. Kirby, D. Beak and D. Chittleborough, Solubility and Batch Retention of CeO2 Nanoparticles in Soils, *Environ. Sci. Technol.*, 2011, **45**(7), 2777–2782.

53 J. Li, R. V. Tappero, A. S. Acerbo, H. Yan, Y. Chu and G. V. Lowry, *et al.*, Effect of CeO_2 nanomaterial surface functional groups on tissue and subcellular distribution of Ce in tomato (*Solanum lycopersicum*), *Environ. Sci.: Nano*, 2019, **6**(1), 273–285.

54 S. J. Parkinson, S. Tungsirisurp, C. Joshi, B. L. Richmond, M. L. Gifford and A. Sikder, *et al.*, Polymer nanoparticles pass the plant interface, *Nat. Commun.*, 2022, **13**(1), 7385.

55 P. Zhang, Y. Ma, C. Xie, Z. Guo, X. He and E. Valsami-Jones, *et al.*, Plant species-dependent transformation and translocation of ceria nanoparticles, *Environ. Sci.: Nano*, 2019, **6**(1), 60–67.

56 H. Sharifan, X. Wang and X. Ma, Impact of nanoparticle surface charge and phosphate on the uptake of coexisting cerium oxide nanoparticles and cadmium by soybean (Glycine max. (L.) merr.), *Int. J. Phytorem.*, 2020, **22**(3), 305–312.

57 H. J. de Almeida, V. M. Vergara Carmona, M. Ferreira Inocêncio, A. E. Furtini Neto, A. B. Cecílio Filho and M. Mauad, Soil Type and Zinc Doses in Agronomic Biofortification of Lettuce Genotypes, *Agronomy*, 2020, **10**(1), 124.

58 USDA, *FoodData Central [Internet]*, 2019, [cited 2024 Aug 15], available from: **https://fdc.nal.usda.gov/fdc-app.html#/food-details/169248/nutrients**.

59 S. S. Dhaliwal, R. K. Naresh, A. Mandal, R. Singh and M. K. Dhaliwal, Dynamics and transformations of micronutrients in agricultural soils as influenced by organic matter build-up: A review, *Environ. Sustain. Indic.*, 2019, **1–2**, 100007.

60 S. K. Ghosh and T. Bera, in *Advances in Nano-Fertilizers and Nano-Pesticides in Agriculture [Internet]*, ed. S. Jogaiah, H. B. Singh, L. F. Fraceto and R. de Lima, Woodhead Publishing, 2021, ch. 22 - Molecular mechanism of nano-fertilizer in plant growth and development: A recent account, pp. 535–60, (Woodhead Publishing Series in Food Science, Technology and Nutrition), available from: **https://www.sciencedirect.com/science/article/pii/B9780128200926000227**.

61 S. Singh, T. Dosani, A. S. Karakoti, A. Kumar, S. Seal and W. T. Self, A phosphate-dependent shift in redox state of cerium oxide nanoparticles and its effects on catalytic properties, *Biomaterials*, 2011, **32**(28), 6745–6753.

62 Y. Li, X. He, J. J. Yin, Y. Ma, P. Zhang and J. Li, *et al.*, Acquired Superoxide-Scavenging Ability of Ceria Nanoparticles, *Angew. Chem., Int. Ed.*, 2015, **54**(6), 1832–1835.

63 S. I. L. Gomes, G. Caputo, N. Pinna, J. J. Scott-Fordsmand and M. J. B. Amorim, Effect of 10 different TiO2 and ZrO2 (nano)materials on the soil invertebrate Enchytraeus crypticus, *Environ. Toxicol. Chem.*, 2015, **34**(10), 2409–2416.

64 P. Zhang, Z. Guo, Z. Zhang, H. Fu, J. C. White and I. Lynch, Nanomaterial Transformation in the Soil–Plant System: Implications for Food Safety and Application in Agriculture, *Small*, 2020, **16**(21), 2000705.

65 H. Wang, A. S. Adeleye, Y. Huang, F. Li and A. A. Keller, Heteroaggregation of nanoparticles with biocolloids and geocolloids, *Adv. Colloid Interface Sci.*, 2015, **226**, 24–36.

66 C. Mahr, J. Stahl, B. Gerken, V. Baric, M. Frei and F. F. Krause, *et al.*, Characterization of mixing in nanoparticle hetero-aggregates by convolutional neural networks, *Nano Sel.*, 2024, **5**(4), 2300128.

67 A. Praetorius, E. Badetti, A. Brunelli, A. Clavier, J. Alberto Gallego-Urrea and A. Gondikas, *et al.*, Strategies for determining heteroaggregation attachment efficiencies of engineered nanoparticles in aquatic environments, *Environ. Sci.: Nano*, 2020, **7**(2), 351–367.